American Mineralogist, Volume 95, pages 1172–1181, 2010

Elbrusite-(Zr)—A new uranian garnet from the Upper Chegem caldera, Kabardino-Balkaria, Northern Caucasus, Russia

Irina O. Galuskina,[1,*] Evgeny V. Galuskin,[1] Thomas Armbruster,[2] Biljana Lazic,[2] Joachim Kusz,[3] Piotr Dzierżanowski,[4] Viktor M. Gazeev,[5] Nikolai N. Pertsev,[5] Krystian Prusik,[6] Aleksandr E. Zadov,[7] Antoni Winiarski,[3] Roman Wrzalik,[3] and Anatoly G. Gurbanov[5]

[1]Faculty of Earth Sciences, Department of Geochemistry, Mineralogy and Petrography, University of Silesia, Będzińska 60, 41-200 Sosnowiec, Poland
[2]Mineralogical Crystallography, Institute of Geological Sciences, University of Bern, Freiestrasse 3, CH-3012 Bern, Switzerland
[3]August Chełkowski Institute of Physics, University of Silesia, Uniwersytecka 4, 40-007 Katowice, Poland
[4]Institute of Geochemistry, Mineralogy and Petrology, University of Warsaw, al. Żwirki i Wigury 93, 02-089 Warszawa, Poland
[5]Institute of Geology of Ore Deposits, Petrography, Mineralogy and Geochemistry (IGEM), Russian Academy of Sciences, Staromonetny 35, 119017 Moscow, Russia
[6]Institute of Materials, University of Silesia, Uniwersytecka 4, 40-007 Katowice, Poland
[7]OOO Science-Research Center NEOCHEM, Dmitrovskoye Highway 100/2, 127238 Moscow, Russia

Abstract

Elbrusite-(Zr) $Ca_3(U^{6+}Zr)(Fe^{3+}_2Fe^{2+})O_{12}$, a new uranian garnet ($Ia\bar{3}d$, $a \approx 12.55$ Å, $V \approx 1977$ Å^3, $Z = 8$), within the complex solid solution elbrusite-kimzeyite-toturite $Ca_3(U,Zr,Sn,Ti,Sb,Sc,Nb...)_2(Fe,Al,Si,Ti)_3O_{12}$ was discovered in spurrite zones in skarn xenoliths of the Upper Chegem caldera. The empirical formula of holotype elbrusite-(Zr) with 25.14 wt% UO_3 is $(Ca_{3.040}Th_{0.018}Y_{0.001})_{\Sigma 3.059}(U^{6+}_{0.658}Zr_{1.040}Sn_{0.230}Hf_{0.009}Mg_{0.004})_{\Sigma 1.941}(Fe^{3+}_{1.575}Fe^{2+}_{0.559}Al_{0.539}Ti^{4+}_{0.199}Si_{0.099}Sn_{0.025}V^{5+}_{0.004})_{\Sigma 3}O_{12}$. Associated minerals are spurrite, rondorfite, wadalite, kimzeyite, perovskite, lakargiite, ellestadite-(OH), hillebrandite, afwillite, hydrocalumite, ettringite group minerals, and hydrogrossular. Elbrusite-(Zr) forms grains up to 10–15 μm in size with dominant {110} and minor {211} forms. It often occurs as zones and spots within Fe^{3+}-dominant kimzeyite crystals up to 20–30 μm in size. The mineral is dark-brown to black with a brown streak. The density calculated on the basis of the empirical formula is 4.801 g/cm^3 The following broad bands are observed in the Raman spectra of elbrusite-(Zr): 730, 478, 273, 222, and 135 cm^{-1}. Elbrusite-(Zr) is radioactive and nearly completely metamict. The calculated cumulative dose (α-decay events/mg) of the studied garnets varies from 2.50×10^{14} [is equivalent to 0.04 displacement per atom (dpa)] for uranian kimzeyite (3.36 wt% UO_3), up to 2.05×10^{15} (0.40 dpa) for elbrusite-(Zr) with 27.09 wt% UO_3.

Keywords: Elbrusite-(Zr), new garnet, uranium, solid solution, metamictization, Raman spectroscopy, EBSD, Upper Chegem caldera

Introduction

Uranium contents in natural garnets have been analyzed only in trace amounts (Lupini et al. 1992; Smith et al. 2004; Gaspar et al. 2008). Exceptions are garnets containing up to 3 wt% UO_3 belonging to the solid-solution series kimzeyite-schorlomite $Ca_3(Zr,Ti)_2(Fe,Al)_2SiO_{12}$–toturite $Ca_3Sn_2Fe_2SiO_{12}$–bitikleite-(SnAl), and bitikleite-(ZrFe) $Ca_3Sb(Zr,Sn)(Fe,Al)_3O_{12}$, which were recently discovered in cuspidine zones in skarn xenoliths within ignimbrites of the Upper Chegem caldera, Kabardino-Balkaria, Northern Caucasus, Russia (Galuskina et al. 2010a, 2010b). Garnets with U contents up to 27 wt% (0.72 U pfu) UO_3 are found in the spurrite zones of the largest xenolith (xenolith no. 1 of Gazeev at al. 2006; Galuskin et al. 2009). Study of these garnets led to the description of the first natural uranian garnet named elbrusite-(Zr) with the end-member crystal chemical formula $Ca_3(U^{6+}Zr)(Fe^{3+}_2Fe^{2+})O_{12}$. Mineral and name were approved by CNMCN IMA in October 2009 (IMA2009-051).

Uranian ferrigarnets have been synthesized and investigated as a matrix for the immobilization of high-level radioactive waste. Synthetic garnet close in composition to elbrusite-(Zr) has been described in porous ceramics associated with Ca-Al-ferrite and $Zr(Ca,U,Fe)O_2$ (Utsunomiya et al. 2002b). That garnet, containing 20.5 wt% UO_2 and having cell parameter $a \approx$ 13.1 Å, could only be indirectly studied because of its small size (<10 μm). Unfortunately, Utsunomiya et al. (2002b) presented a chemical analysis of this garnet without crystal-chemical formula. Even if the valence of U and Fe remains unknown, two possible variants of crystal-chemical formulae based on 12 O may be derived: (1) $Ca_{2.93}(Zr_{1.52}U^{6+}_{0.54})(Fe^{3+}_{1.64}Fe^{2+}_{0.20}Al_{1.17})O_{12}$ and (2) $Ca_{2.93}(Zr_{1.52}U^{6+}_{0.34}U^{5+}_{0.20})(Fe^{3+}_{1.84}Al_{1.17})O_{12}$. These formulae show that hexavalent U prevails in the composition of the synthetic garnet. In ferrigarnets synthesized in the system CaO-Fe_2O_3-Al_2O_3-SiO_2-ZrO_2-Gd_2O_3-UO_2 at 1400–1500 °C (Yudintsev et al. 2002; Yudintsev 2003), U is incorporated at both polyhedral (X) and octahedral (Y) sites. The authors give two approximate crystal-chemical formulae (not charge-balanced) assigning U: (1) to the polyhedral X site $(Ca_{2.7}U_{0.3})_{\Sigma 3}(Zr_{1.7}Fe_{0.3})_{\Sigma 2}(Al_{1.1}Fe_{1.9})_{\Sigma 3}O_{12}$ [$a = 12.6(1)$ Å], and (2) to the octahedral Y site $(Cd_{2.5}Ca_{0.5})_{\Sigma 3}$

* E-mail: irina.galuskina@us.edu.pl

$(Fe_{1.5}Gd_{0.3}U_{0.2})(Al_1Fe_2)O_{12}$ [a = 12.4(1) Å]. The valence of U and Fe were not determined in these synthetic U-bearing Ca-Cd-ferrigarnets. Considering ionic radii (Shannon 1976), U^{4+} (1 Å) prefers the 8-coordinated X site, whereas the radii of U^{5+} (0.76 Å) and U^{6+} (0.73 Å) are more appropriate for the octahedral Y site.

The end-member elbrusite-(Zr) is Si-free and should be formally classified as an oxide. However, elbrusite-(Zr) forms a complex solid solution with silicate garnets: kimzeyite, toturite, schorlomite; thus, it was assigned to the garnet group. The same principle was used for the classification of the end-members of the bitikleite series, formally ferrites and aluminates (Galuskina et al. 2010b). The end-member formula of elbrusite-(Zr) can be derived from Fe^{3+}-dominant kimzeyite $Ca_3Zr_2Fe_2^{3+}SiO_{12}$ by substituting half of Zr according to the scheme: $^{VI}Zr^{4+}\,^{IV}Si^{4+} \rightarrow {}^{VI}U^{6+}\,{}^{IV}Fe^{2+}$. A Levinson-type modifier is used for specifying uranian garnets (Levinson 1966). The suffix (Zr) indicates the dominant cation at half of the Y sites: elbrusite-(Zr)–$Ca_3U^{6+}ZrFe_2^{3+}Fe^{2+}O_{12}$. The stannian analog ["elbrusite-(Sn)"] was found together with elbrusite-(Zr) in the same skarn.

The name elbrusite-(Zr) was chosen after the highest peak in Europe—Elbrus (5642 m), Northern Caucasus, Russia. The xenoliths with the new garnet are embedded in ignimbrites of the Elbrus-Kyugen volcanic area (Borsuk 1968). The holotype sample of elbrusite-(Zr) is deposited in the Fersman Mineralogical Museum in Moscow, catalog no. 3840/1. In this paper, a description of the first natural uranian garnet elbrusite-(Zr) is presented.

Analytical methods

The morphology and composition of the garnets was investigated using a Philips/FEI ESEM XL30/EDAX scanning electron microscope (Faculty of Earth Sciences, University of Silesia) and a CAMECA SX100 electron-microprobe analyzer (Institute of Geochemistry, Mineralogy and Petrology, University of Warsaw) at 15 kV and 40–50 nA, beam diameter 1–3 μm, using natural and synthetic standards: Mg$K\alpha$ = diopside; Al$K\alpha$ = orthoclase; Si$K\alpha$, Ca$K\alpha$ = wollastonite; Sc$K\alpha$ = Sc; Ti$K\alpha$ = rutile; V$K\alpha$ = V_2O_5; Cr$K\alpha$ = Cr_2O_3; Fe$K\alpha$ = hematite; Sr$L\alpha$ = $SrTiO_3$; Y$L\alpha$ = YAG; Zr$L\alpha$ = zircon; Nb$L\alpha$ = Nb; Sn$L\alpha$ = cassiterite; Sb$L\alpha$ = GaSb; Hf$M\alpha$ = Hf; Th$M\alpha$ = ThO_2; U$M\beta$ = syn. UO_2.

The small size of the garnet crystals required single-crystal electron back-scatter diffraction (EBSD) analysis for determination of the cell dimensions and symmetry. EBSD images were recorded with a HKL EBSD system on JSM-6480 (Institute of Materials Science, University of Silesia) using a 30 kV beam. Calibration of the geometry of the SEM and EBSD system was carried out on Si for two detector distances (DD), i.e., 177 mm (normal working position) and 150 mm (camera refracted position). The program "Channel5" (Oxford Instruments) was used for interpretation of the EBSD diffraction patterns.

Single crystals of uranian garnet were also investigated with an APEX II SMART diffractometer (University of Bern), Mo$K\alpha$ $\lambda = 0.71073$ Å obtained at 50 kV, 35 mA. A powdered sample was examined with a D/max RAPID II X-ray diffractometer from Rigaku (Institute of Physics, University of Silesia) with a rotating anode, Ag$K\alpha$ radiation operated at 60 kV and 200 mA, equipped with a $K\alpha$ monochromator and curved imaging plate systems for 2D X-ray scattering.

Raman spectra of single garnet crystals were recorded using a LabRAM HR800 (Jobin-Yvon-Horiba, Wrocław University of Technology). The Raman spectra were recorded in 0° degree geometry, in the range of 50–4000 cm^{-1} Raman shift and with a spectral resolution of 2.5 cm^{-1}. The collection time was 10 s and 16 scans were accumulated.

Results

Elbrusite-(Zr) was found in a spurrite zone of xenolith no. 1 in ignimbrites of the Upper Chegem caldera close to the Lakargi peak on the interfluve between the Chegem and Kenstanty Rivers in the Northern Caucasus (Gazeev et al. 2006). Xenolith no. 1 is more than 20 m across and shows a pronounced zoned structure. From the center to the rim, the following zones are distinguished: (1) brucite (-periclase) calcite marble; (2) spurrite zone; (3) Ca-humites zone (reinhardbraunsite, kumtyubeite, chegemite); and (4) cuspidine zone replacing a larnite zone at the contact with the ignimbrites (Galuskin et al. 2009). Thin wollastonite, rustumite, and rankinite zones occur at the endocontact with the ignimbrite. Wadalite, rondorfite, ellestadite-(OH), perovskite, srebrodolskite, magnesioferrite, and lakargiite are widespread in different rock types within xenolith 1. Hillebrandite, afwillite, minerals of the ettringite group, hydrocalumite, and hydrogarnets of the katoite-hibschite series are more common among secondary low-temperature minerals. Rare and new minerals associated with elbrusite-(Zr) are listed in Table 1[1].

[1] Deposit item AM-10-034; Tables 1 and 3–6, Figure 4, and CIF. Deposit items are available two ways: For a paper copy contact the Business Office of the Mineralogical Society of America (see inside front cover of recent issue) for price information. For an electronic copy visit the MSA web site at http://www.minsocam.org, go to the *American Mineralogist* Contents, find the table of contents for the specific volume/issue wanted, and then click on the deposit link there.

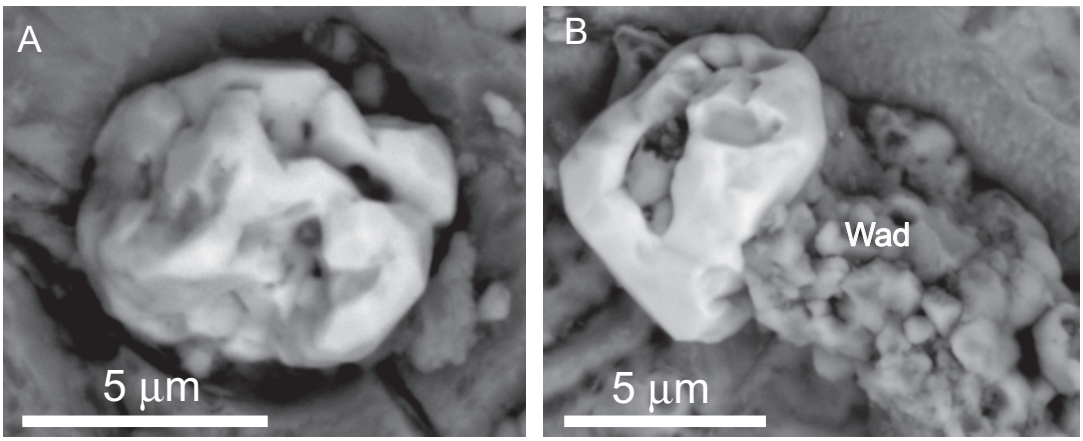

Figure 1. BSE image of elbrusite-(Zr) morphology: (**a**) {110} and {211} forms of a skeletal crystal, (**b**) {211} forms of a skeletal crystal intergrown with wadalite (Wad).

TABLE 2. Chemical composition and calculated α-decay cumulative dose of uranium garnets from altered xenoliths

	1			2	3	4	5	6	7	8	9	10	11	12	13	14	15	16	17
UO_3 wt%	25.14	1.10	23.5–26.55	3.36	8.14	10.19	15.13	15.29	16.88	20.60	23.71	23.99	26.55	27.09	17.32	23.91	9.13	13.30	19.21
Sb_2O_5	n.d.			n.d.	n.d.	n.d.	n.d.	n.d.	n.d.	n.d.	n.d.	n.d.	n.d.	n.d.	1.02	0.45	n.d.	0.52	0.49
Nb_2O_5	n.d.			n.d.	0.25	0.09	0.11	n.d.	0.14	0.06	0.13	0.29	n.d.	0.10	0.12	0.19	0.77	0.48	0.24
V_2O_5	0.05	0.05	0–0.12	n.d.	n.d.	n.d.	n.d.	n.d.	n.d.	n.d.	n.d.	0.06	n.d.	n.d.	n.d.	n.d.	n.d.	n.d.	0.05
ThO_2	0.65	0.08	0.51–0.77	n.d.	n.d.	n.d.	0.23	n.d.	n.d.	n.d.	0.04	n.d.	0.67	n.d.	n.d.	n.d.	0.59	0.11	0.10
HfO_2	0.25	0.04	0.19–0.29	0.65	0.50	0.48	0.53	0.30	0.33	0.49	0.42	n.d.	0.19	0.24	0.46	0.32	0.50	0.38	0.30
SnO_2	5.13	0.34	4.78–5.60	5.93	6.18	4.34	3.05	6.88	7.02	3.57	3.12	22.12	4.78	4.47	0.92	0.83	4.34	4.96	4.62
ZrO_2	17.11	0.65	16.32–18.14	30.43	27.22	27.27	25.13	21.2	20.77	21.64	20.17	1.38	16.65	17.16	25.03	19.38	25.17	21.46	19.43
TiO_2	2.12	0.24	1.81–2.45	6.67	4.76	5.27	4.16	4.85	3.80	3.34	2.71	2.86	1.81	2.15	2.95	3.07	5.12	3.90	2.82
SiO_2	0.79	0.14	0.57–1.00	4.10	3.65	3.00	1.57	2.55	2.16	1.16	0.78	1.22	0.57	0.63	2.29	1.79	4.61	4.25	2.60
Al_2O_3	3.67	0.23	3.45–4.08	3.90	4.44	2.93	2.77	2.84	3.22	2.97	2.92	2.18	3.51	3.55	4.98	4.79	3.65	3.70	3.50
Sc_2O_3	n.d.			1.03	0.12	0.16	n.d.	0.19	0.13	n.d.	0.02	0.08	n.d.	n.d.	0.07	0.10	0.18	0.16	0.09
Cr_2O_3		0.02	0–0.03	n.d.	n.d.	0.03	0.02	n.d.	n.d.	0.03	n.d.	n.d.	n.d.	n.d.	n.d.	n.d.	n.d.	n.d.	n.d.
Y_2O_3	0.02	0.02	0–0.04	n.d.	n.d.	n.d.	0.44	n.d.	n.d.	n.d.	0.11	n.d.	n.d.	n.d.	n.d.	n.d.	n.d.	n.d.	0.03
Fe_2O_3	16.80	0.28	16.35–17.10	18.01	16.52	19.57	19.88	19.29	18.39	18.57	17.65	18.28	16.33	15.24	15.33	14.73	18.38	17.41	17.66
FeO	5.36	0.28	5.15–5.48	0.27	1.56	1.53	2.83	2.81	3.32	4.26	5.4	4.73	6.01	6.54	4.28	5.43	2.38	3.27	4.10
SrO	n.d.			n.d.	n.d.	n.d.	n.d.	n.d.	n.d.	n.d.	n.d.	n.d.	n.d.	n.d.	>0.1	>0.1	n.d.	0.13	0.10
CaO	22.76	0.31	22.25–23.24	26.50	25.35	25.53	23.93	24.87	24.26	23.60	22.93	22.74	22.25	22.51	23.72	23.34	25.38	24.35	23.68
MgO	0.02	0.01	0–0.03	n.d.	n.d.	n.d.	n.d.	n.d.	0.02	n.d.	n.d.	n.d.	0.02	0.03	n.d.	n.d.	n.d.	0.04	0.02
Total	99.87			100.85	98.69	100.39	99.78	101.08	100.44	100.36	100.11	99.93	99.34	99.71	98.49	98.33	100.20	98.42	99.03
Ca*	3.040			3.033	3.053	3.070	3.013	3.063	3.050	3.042	3.026	3.104	3.024	3.039	3.001	3.047	3.001	3.002	3.034
Th	0.018						0.006				0.001		0.019				0.015	0.003	0.003
Y	0.001						0.027				0.007								0.002
Sr																		0.009	0.007
X site	3.059			3.033	3.053	3.070	3.046	3.063	3.050	3.042	3.034	3.104	3.043	3.039	3.001	3.047	3.016	3.014	3.046
U^{6+}	0.658			0.075	0.192	0.240	0.373	0.369	0.416	0.521	0.614	0.642	0.708	0.717	0.430	0.612	0.212	0.321	0.482
Nb^{5+}					0.013	0.005	0.006		0.007		0.007	0.017		0.006	0.006	0.010	0.038	0.025	0.013
Sb^{5+}															0.045	0.020		0.022	0.022
Zr	1.040			1.585	1.492	1.492	1.440	1.188	1.188	1.269	1.212	0.086	1.030	1.054	1.441	1.151	1.355	1.204	1.133
Sn	0.230			0.191	0.221	0.160	0.115	0.315	0.311	0.144	0.116	1.124	0.208	0.169	0.044	0.040	0.191	0.228	0.220
Ti^{4+}								0.036				0.018			0.002	0.090	0.156	0.150	0.061
Hf	0.009			0.020	0.016	0.015	0.018	0.010	0.011	0.017	0.015		0.007	0.009	0.016	0.011	0.016	0.012	0.010
Sc				0.096	0.012	0.015		0.019	0.013		0.002	0.009			0.007	0.011	0.017	0.016	0.009
Cr^{3+}						0.003	0.002			0.003									
Mg	0.004								0.003				0.004	0.006				0.007	0.004
Y site	1.941			1.967	1.946	1.930	1.954	1.937	1.949	1.954	1.966	1.896	1.957	1.961	1.991	1.945	1.985	1.985	1.954
Si	0.099			0.438	0.410	0.337	0.184	0.293	0.253	0.140	0.096	0.155	0.072	0.079	0.271	0.218	0.509	0.489	0.311
Al	0.539			0.491	0.588	0.388	0.384	0.385	0.445	0.421	0.424	0.327	0.525	0.527	0.693	0.688	0.475	0.502	0.493
Fe^{3+}	1.575			1.448	1.397	1.653	1.758	1.669	1.623	1.684	1.635	1.753	1.558	1.445	1.369	1.357	1.526	1.507	1.588
Fe^{2+}	0.559			0.025	0.147	0.143	0.278	0.270	0.326	0.426	0.557	0.504	0.638	0.689	0.407	0.546	0.221	0.315	0.411
Ti^{4+}	0.199			0.536	0.402	0.445	0.368	0.383	0.336	0.302	0.251	0.256	0.173	0.204	0.260	0.191	0.269	0.187	0.193
Sn	0.025			0.062	0.056	0.034	0.028		0.017	0.027	0.037		0.034	0.056					
V^{5+}	0.004											0.005							0.004
Z site	3.000			3.000	3.000	3.000	3.000	3.000	3.000	3.000	3.000	3.000	3.000	3.000	3.000	3.000	3.000	3.000	3.000
$D\alpha \times 10^{14}$	19.14			2.50	6.23	7.66	11.45	11.43	12.70	15.54	17.91	18.14	20.33	20.52	13.30	18.38	7.01	10.22	14.66
dpa	0.37			0.04	0.11	0.14	0.21	0.21	0.23	0.29	0.35	0.36	0.40	0.40	0.24	0.34	0.12	0.18	0.27

Notes: 1–12 = xenolith no. 1: 1 = holotype specimen of elbrusite-(Zr), mean 6; 2–7 = uranian Fe^{3+}-dominant kimzeyite (7 = mean from 5, crystal used for single-crystal XRD); 8–12 = elbrusite series: 8,9,11,12 = elbrusite-(Zr), 10 = "elbrusite-(Sn);" 13,14 = xenolith no. 7: 13 = uranian kimzeyite from kimzeyite-lakargiite aggregate used for μXRD powder diffraction, 14 = elbrusite-(Zr); 15–17 = xenolith no. 3: 15 = uranian kimzeyite used for single-crystal XRD, 16 = uranian kimzeyite, 17 = elbrusite-(Zr). Analysis points 3, 4, 6, 8–11, 13, 16, 17 shown in Figure 1 and analysis point 5 shown in Figure 3d. n.d. = not detected. $D\alpha$ = cumulative dose of α-decay events/mg, dpa = displacement per atom. * = calculated on 12 O, Fe^{3+}/Fe^{2+} calculated from charge balance.

Elbrusite-(Zr) and uranian kimzeyite form small crystals of skeletal structure with {110} and {211} faces. Larger grains are generally irregular and up to 20–30 μm in size (Figs. 1 and 2). Small (<10 μm) relatively homogeneous crystals of elbrusite-(Zr) with imperfect form are confined to fine-grained aggregates of wadalite-filled openings between spurrite grains (Fig. 2a; Table 2, analyses 1, 11). Small elbrusite-(Zr) crystals, up to 10–15 μm in size, also overgrow lakargiite aggregates (Fig. 2b; Table 2, analyses 8, 9). Elbrusite-(Zr) and its stannian analog form irregular zones and spots in Fe^{3+}-dominant kimzeyite (Figs. 2c and 2d; Table 2, analyses 3, 4, 6, 10). There is a general trend of increasing U content toward the crystal rims. Single findings of elbrusite-(Zr) and high-U kimzeyite have also been made in cuspidine zones in xenoliths no. 3 and 7 [Fig. 2e and 2f; Table 2, analyses 13, 16, 17; see Galuskin et al. (2009) for a geological sketch with the localities of the xenoliths mentioned].

The color of elbrusite-(Zr) crystals is brown, dark-brown to black with a brown streak. Metamict high-U garnet is translucent, whereas garnets with compositions at the kimzeyite-elbrusite boundary are transparent. Elbrusite-(Zr) has a glassy to dull, resinous luster. Refractive index, density, and microhardness were not determined because of the small size and skeletal structure of the elbrusite-(Zr). Cleavage is absent. Fracture is irregular. The calculated density on the basis of the empirical formula is 4.801 g/cm^3. The mineral does not show fluorescence and is radioactive.

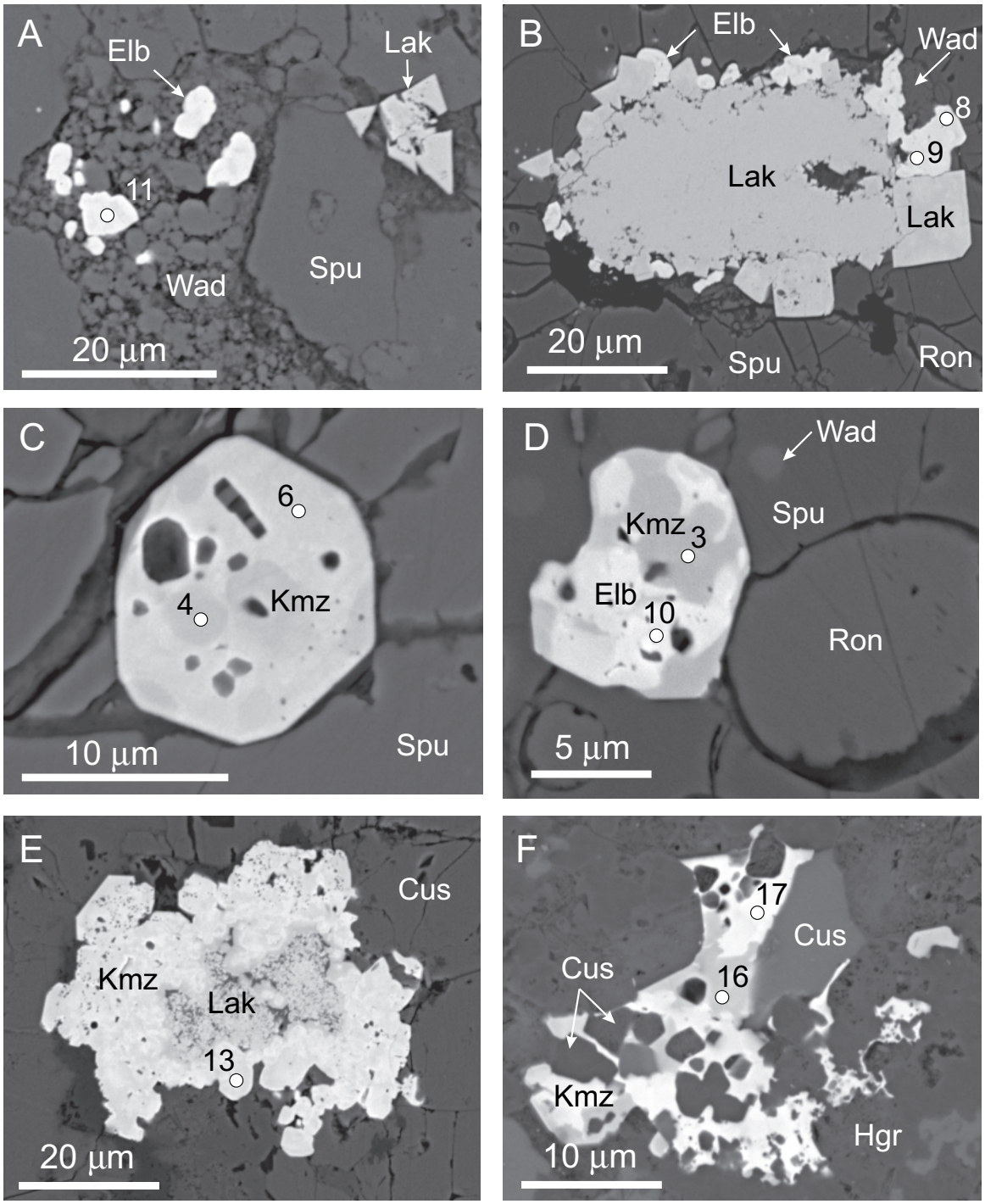

Figure 2. (**a**) Elbrusite-(Zr) grains in aggregates of wadalite. (**b**) Elbrusite-(Zr) overgrowing lakargiite. (**c**) {110} forms with minor {211} forms of uranian kimzeyite. (**d**) Inhomogeneous crystal of "elbrusite-(Sn)"-kimzeyite. (**e**) Lakargiite-kimzeyite aggregate (xenolith no. 7). (**f**) "Poikilitic" grain of uranian kimzeyite (xenolith no. 3). Cus = cuspidine, Elb = elbrusite, Hgr = hibschite, Lak = lakargiite, Ron = rondorfite, Kmz = kimzeyite, and Wad = wadalite.

Diffraction investigations of elbrusite-(Zr) using EBSD show that the mineral is nearly completely metamict. Its amorphous state is supported by the absence of Kikuchi lines in the EBSD pattern (Fig. 3a) obtained for point 9 shown in Figure 2b. In contrast, uranian lakargiite (perovskite structure-type) with 7 wt% of UO_3, coexisting with elbrusite-(Zr) (Fig. 2b) is crystalline: a = 5.59, b = 5.76, c = 8.02 Å (*Pnma*), MAD = 0.57° [Figs. 3b and 3c; initial structural data from Koopmans et al. (1983)]. In addition, in the same thin section, an EBSD pattern was obtained for high-U (ca. 15 wt% UO_3) Fe^{3+}-dominant kimzeyite (Figs. 3d–3f; Table 2, analysis 5). Fitting the EBSD pattern for DD = 177 mm to a garnet model with a = 12.55 Å yielded MAD = 0.25° (excel-

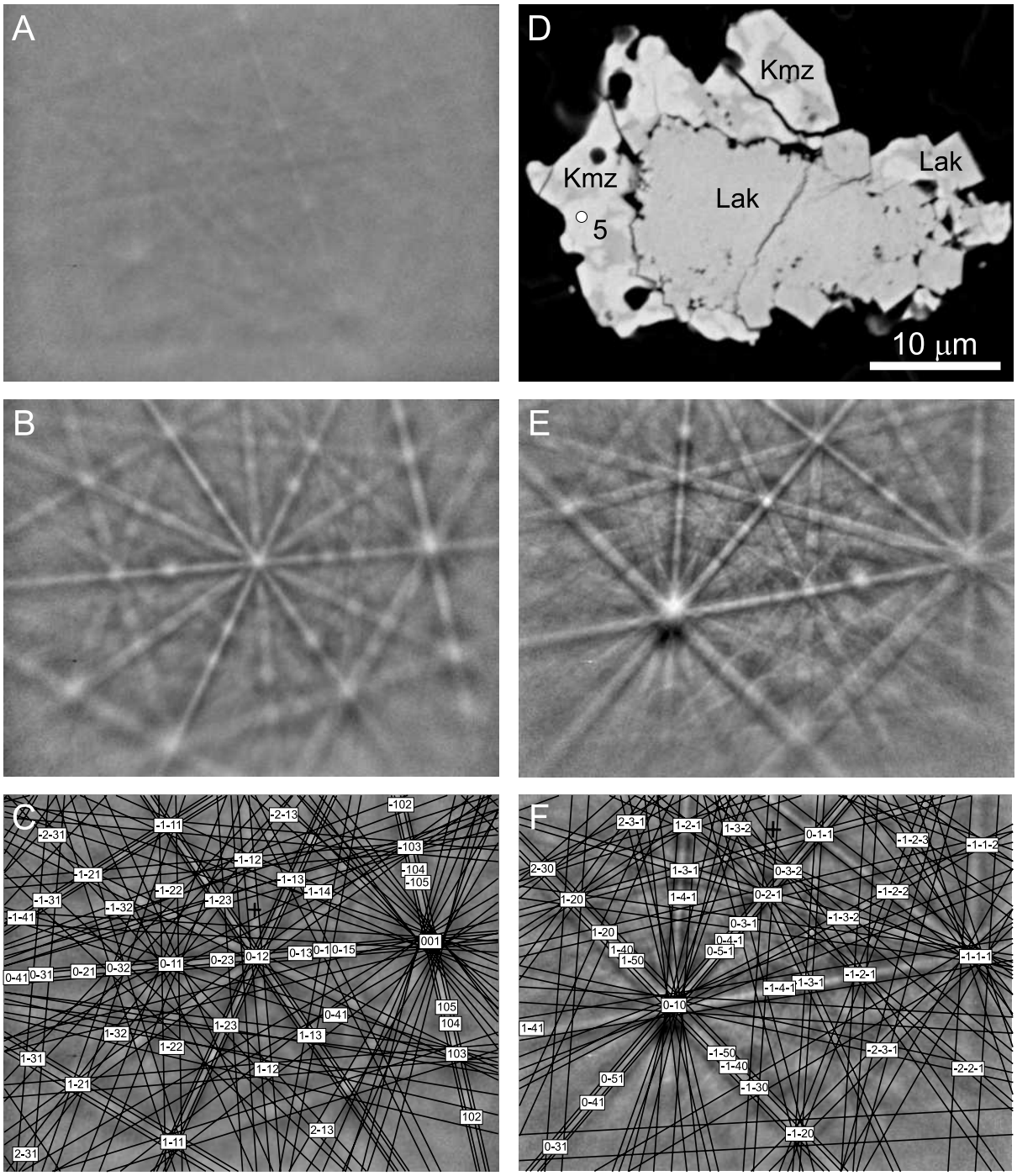

FIGURE 3. (**a**) EBSD pattern of elbrusite-(Zr) obtained for point 9 shown in Figure 2b. (**b–c**) EBSD pattern (**b**) and fitting result (**c**) of lakargiite, cubic crystal shown in Figure 2b near point 9. (**d**) Uranian kimzeyite (Kmz) overgrowing an aggregate of lakargiite (Lak). (**e–f**) EBSD pattern (**e**) and fitting result (**f**) obtained for point 5 shown in **d**.

lent fit). The unit-cell parameter obtained by EBSD is close to a = 12.5965(5) Å of U-bearing Fe^{3+}-dominant kimzeyite from xenolith no. 3, which was studied with a single-crystal X-ray diffractometer (Table 2, analysis 15; Tables 3–6[1]). Due to the similar ionic radii [^{VI}Zr 0.72 and $^{VI}U^{6+}$ 0.73 Å; Shannon (1976)], the cell parameter of elbrusite-(Zr) is approximately the same as that of U-rich kimzeyite.

As recognized in EBSD experiments, elbrusite-(Zr) with UO_3 contents higher than 20 wt% is nearly completely metamict. Thus, we collected X-ray single-crystal diffraction data for a uranian garnet 23 × 22 × 16 μm in size [a = 12.7456(9) Å, V = 2070.5(3) Å^3], with a composition corresponding to the elbrusite-kimzeyite boundary (≈17% UO_3: Table 2, analysis 7). Unfortunately, the high degree of metamictization and the small crystal size did not allow a high-quality structure refinement. As a compromise, a crystal of uranian kimzeyite with ≈10 wt%

UO_3 (Table 2, analysis 15) was used for single-crystal X-ray data collection and subsequent structure refinement (deposit item: Tables 3–6[1]).

Powder X-ray diffraction data for the aggregate of high-U Fe^{3+}-kimzeyite [43% of the elbrusite-(Zr) end-member] and lakargiite shown in Figure 2e (Table 2, analysis 13) were collected. In spite of the small amount of material available, and the partial metamictization of the garnet, the cell dimension could be determined from a few diffraction maxima: a = 12.75(3) (*Ia3d*) Å, V = 2072.7(3) Å^3 (Fig. 4[1]).

Calculation of predicted cell parameters of garnet according to the equation (Strocka et al. 1978): $a = b_1+b_2r_X+b_3r_Y+b_5r_Xr_Y+b_6r_Xr_Z+b_4r_Z$ (Å), where b_1 = 7.02954; b_2 = 3.31277; b_3 = 2.49398; b_4 = 3.34124; b_5 = –0.87758; b_6 = –1.38777; and r_X, r_Y, r_Z = weight-average effective ionic radii (Shannon 1976) of cations X, Y, and Z, respectively, indicates that predicted cell parameters for elbrusite-(Zr) (Table 2, analysis 7) and uranian kimzeyite (Table 2, analysis 15), respectively, are smaller than the experimental ones: elbrusite-(Zr): a_{cal} = 12.58 Å and a_{exp} = 12.7456(9) (difference in cell volume: 3.9%); uranian kimzeyite: a_{cal} = 12.53 Å and a_{exp} = 12.5965(5) (difference in cell volume: 1.7%). An increase in cell volume (decrease in density) usually accompanies the metamictization process (Wülser et al. 2005). Radiation-induced amorphization of coeval uranian garnets from altered xenoliths of Upper Chegem caldera depends on the U concentration. The cumulative dose (α-decay events/mg) for garnet compositions represented in Table 2 was calculated using following equation (Ewing et al. 2000): $D\alpha = 8N_1[\exp(\lambda_1 t) - 1] + 7N_2[\exp(\lambda_2 t) - 1] + 6N_3[\exp(\lambda_3 t) - 1]$, where N_1, N_2, N_3 are the actual values of ^{238}U, ^{235}U, and ^{232}Th, respectively, in atoms/mg; λ_1, λ_2, and λ_3 are the decay constants for ^{238}U, ^{235}U, and ^{232}Th, respectively, in years^{-1}; and t is the estimated age (in years) of the ignimbrites [~2.8 Ma according to Lipman et al. (1993), Gazis et al. (1995)], coeval with the studied garnets. The final dose expressed in displacement per atom (dpa) is calculated according to the equation: Dose (dpa) = $9.40 \times 10^5 \times D\alpha \times M/(N_A \times 6)$, where M is the molar mass of the garnet and N_A is Avogadro's number. The cumulative dose of the studied garnets varies according to the U content from 2.50 $\times 10^{14}$ α-decay events/mg and 0.04 dpa for uranian kimzeyite with 3.36 wt% UO_3, up to 2.05×10^{15} α-decay events/mg and 0.40 dpa for elbrusite-(Zr) with 27.09 wt% UO_3 (Table 2).

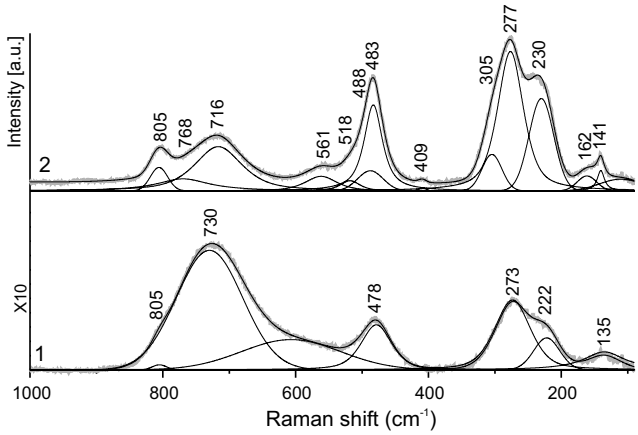

FIGURE 5. Raman spectra: 1 = elbrusite-(Zr) (Table 2, analysis 9; Fig. 2b); 2 = uranian kimzeyite (Table 2, analysis 5; Fig. 3d).

The Raman spectra of elbrusite-(Zr) and uranian kimzeyite resemble those of kimzeyite and toturite (Schingaro et al. 2001; Galuskina et al. 2005, 2010a). High background, blur, and weak band intensities in comparison to U-free kimzeyite are characteristic features of these spectra (Fig. 5). Three spectral regions are distinguished: 650–850 cm^{-1} [$(Z\text{-}O)_{stretch}$], near 500 cm^{-1} [$(Z\text{-}O)_{bend}$], and 270–300 cm^{-1} [$R(ZO_4)$]. Bands below 270 cm^{-1} are related to translational motions of $T(ZO_4)$ and $T(Ca^{2+})$ (Fig. 5). Generally, the bands are shifted toward lower frequencies as described for silicate garnets (Kolesov and Geiger 1998). The broad line centered near 730 cm^{-1} in the elbrusite-(Zr) spectrum is related to $[Fe^{3+}O_4]^{5-}$ vibrations. Its asymmetric nature and significant intensity near 600 cm^{-1} may indicate contributions from $[Fe^{2+}O_4]^{6-}$, $[AlO_4]^{5-}$, and $[TiO_4]^{4-}$ vibrations. In addition, uranyl ions, possibly occurring within metamict domains of elbrusite-(Zr), have $[UO_2]^{2+}$ vibrations in the range 700–900 cm^{-1} (Hoekstra 1965; Liegeois-Duyckaerts 1977; Allen and Griffiths 1979; Frost et al. 2006). The well-resolved line at 805 cm^{-1} in spectra of uranian kimzeyite is related to $[SiO_4]^{4-}$ vibrations.

DISCUSSION

Calcium garnets from high-temperature skarns in the Lakargi area have the complex composition $Ca_3(Zr,Sn,U,Sb,Ti,Sc,Mg)_2(Fe,Si,Al,Ti)_3O_{12}$ with significant variations of elements at both octahedral (Y) and tetrahedral (Z) sites. For the classification of the uranian garnets, we use a triangular diagram with elbrusite $Ca_3U^{6+}(Zr,Sn)(R_2^{3+}Fe^{2+})O_{12}$–toturite $Ca_3Sn_2(R_2^{3+}R^{4+})O_{12}$–kimzeyite-schorlomite $Ca_3(Zr,Ti^{4+})_2(R_2^{3+}R^{4+})O_{12}$ at the corners (Fig. 6). Fields for minerals species are defined in accordance with the "dominant-constituent rule" (Hatert and Burke 2008). Analytical results for the uranian kimzeyites and the elbrusite holotype samples from the spurrite skarns of xenolith no. 1 are completed by those of the uranian garnets from xenoliths no. 3 and 7 (Fig. 6).

The following principles were defined for the determination of a simplified crystal-chemical formula for elbrusite-(Zr): (1) High-temperature skarn minerals from the same locality show maximum calcium content, suggesting that the eight-coordinate X site in all garnets is fully occupied by Ca (furthermore, the host rock is an altered limestone). (2) Uranium is assumed to be U^{6+} as highly oxidizing conditions are also indicated by the new mineral vorlanite $(CaU^{6+})O_4$ associated with elbrusite-(Zr) (Galuskin et al., in preparation). The octahedral Y site in the garnet structure is also suitable for U^{6+} occupation. Hexavalent U requires charge balance by divalent Fe. And (3) considering that the octahedral site in the garnet structure is fully occupied by Zr, Sn, and U (according to chemical analyses), we suggest that Fe^{2+}, Fe^{3+}, and Ti^{4+} occupy the tetrahedral Z site in the garnet structure. The presence of Fe^{2+} is confirmed by a Raman band below 700 cm^{-1}. We suggest a crystal-chemical model for elbrusite in which U^{6+} with ionic radius 0.73 Å (Shannon 1976) occupies the Y site substituting for four-valent cations (Zr [0.72 Å], Sn [0.69 Å]). Charge-balance is obtained by partial incorporation of Fe^{2+} at the Z site according to: $^{VI}Zr^{4+}(Sn^{4+}) + {}^{IV}Si^{4+}(Ti^{4+}) \rightarrow {}^{VI}U^{6+} + {}^{IV}Fe^{2+}$ (Figs. 7 and 8). The positive correlation between U and Ca (usually > 3 apfu), is probably related to the high degree of metamictization characteristic of high-U garnets (Fig. 8). Uranium shows an inverse correlation with Si,

Ti, Zr, and Al, which fits the model (Fig. 7). Uranium and Sn are not correlated. However, U-rich garnets, occurring as spots in U kimzeyite (Fig. 2d), are enriched in Sn. A chemical analysis of the tin analog of elbrusite-(Zr) ["elbrusite-(Sn)"] is given in Table 2 (analysis 10). The formula contains more than 50% of the $Ca_3U^{6+}Sn^{4+}Fe^{3+}_2Fe^{2+}O_{12}$ component. It has a Ca content (Ca 3.1 apfu) exceeding the theoretical value for garnets, which is interpreted as evidence of metamictization. Possibly, Fe^{2+} may also occupy the octahedral Y site and Sn the tetrahedral Z site, but we used toturite $Ca_3Sn_2Fe^{3+}_2SiO_{12}$ with Sn at the Y site as the basic component in the definition of Sn-containing end-members. The small size of elbrusite-(Zr) does not allow the determination of the valence state of the Fe, U, and Ti or to identify the true distribution of Sn, Ti, Fe, and U over the Y and Z sites in the garnet structure. Presence of a small amount of $^{VI}U^{5+}$ (0.76 Å) at the Y site cannot be ruled out, as its ionic radius is close to the one of $^{VI}U^{6+}$ (0.73 Å) (Shannon 1976). Thus, the following substitution scheme can be suggested: $^{VI}U^{6+} + {}^{IV}Fe^{2+} = {}^{VI}U^{5+} + {}^{IV}Fe^{3+}$. Interestingly, valence state determinations of Fe in synthetic ferrite garnets containing significant concentrations of actinides have given contrary results using different methods. Energy loss spectroscopy (EELS) has suggested that ferrous Fe prevails (Utsunomiya et al. 2005), which is in contrast to the expected stoichiometry, whereas ^{57}Fe Mössbauer spectroscopy indicates that Fe is predominantly ferric (Rusakov et al. 2005).

Compositions of garnets belonging to the solid solution elbrusite–kimzeyite-schorlomite–toturite can be expressed by the formula $Ca_3U^{6+}_x(Zr,Sn^{4+},Ti^{4+})_{2-x}R^{3+}_2Fe^{2+}_xR^{4+}_{1-x}O_{12}$, where $0 \le x \le 1$ and R^{3+} = Al, Fe; R^{4+} = Ti, Si. The holotype sample of elbrusite-(Zr) has the formula $(Ca_{3.040}Th_{0.018}Y_{0.001})_{\Sigma 3.059}(U^{6+}_{0.658}Zr_{1.040}Sn_{0.230}Hf_{0.009}Mg_{0.004})_{\Sigma 1.941}(Fe^{3+}_{1.575}Fe^{2+}_{0.559}Al_{0.539}Ti^{4+}_{0.199}Si_{0.099}Sn_{0.025}V^{5+}_{0.004})_{\Sigma 3}O_{12}$. This complex formula can be split into the following components: elbrusite-(Zr) $Ca_3U^{6+}ZrFe^{3+}_2Fe^{2+}O_{12}$ = 60%; $Ca_3U^{6+}_{0.5}Zr_{1.5}Fe^{3+}_3O_{12}$ = 9% (the sum of uranian garnet end-members = 69%); kimzeyite $Ca_3Zr_2R^{3+}_2R^{4+}O_{12}$ = 20%; toturite $Ca_3Sn_2R^{3+}_2R^{4+}O_{12}$ = 10%; $ThCa_2Sn_2R^{3+}_3O_{12}$ = 1%. Addition of the $Ca_3U^{6+}_{0.5}Zr_{1.5}Fe^{3+}_3O_{12}$ component, modified by the possible substitution $R^{2+}_{0.5}R^{4+}_{0.5} \leftrightarrow R^{3+}$, became necessary because the holotype crystal contained more U than ferrous Fe. In the determination diagram, this component plots between kimzeyite and elbrusite-(Zr), dividing the kimzeyite-elbrusite series into two fields (Fig. 6). In elbrusite-(Zr), the amount of $^{IV}R^{4+}$does not exceed 0.3 apfu if $Fe^{2+} > 0.5$ apfu. This confirms the description of the new garnet composition as kimzeyite (+schorlomite, toturite)–elbrusite-(Zr) solid solution. Uranian kimzeyite often exhibits $^{IV}Ti^{4+} > Si$ (Table 2, analyses 2, 4) indicating the presence of a titanian analog of Fe^{3+}-dominant kimzeyite with an ideal formula $Ca_3Zr_2Fe^{3+}_2Ti^{4+}O_{12}$ in nature.

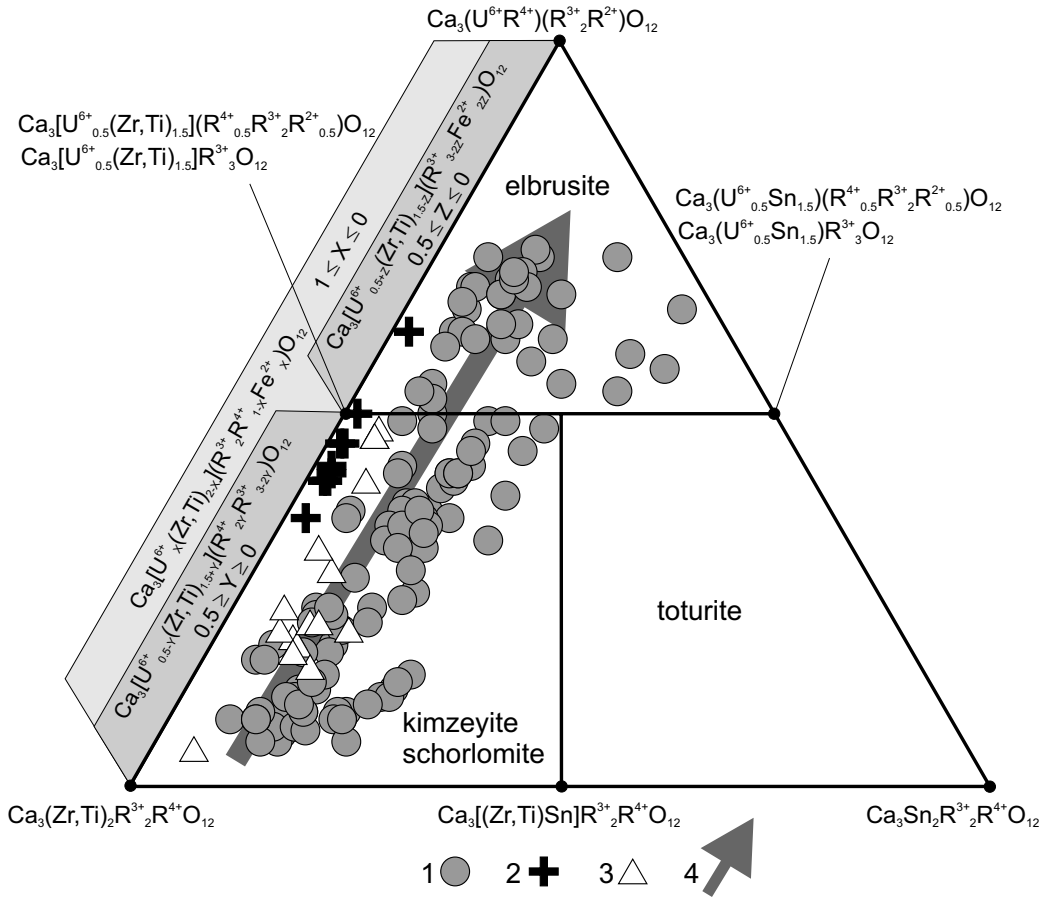

FIGURE 6. Triangular classification diagram kimzeyite-schorlomite–elbrusite–toturite. 1 (gray circles) = garnet compositions in xenolith no. 1; 2 (crosses) = garnet compositions in xenolith no. 7; 3 (triangles) = garnet compositions in xenolith no. 3; 4 (arrow) = general trend of compositional changes in uranian garnets.

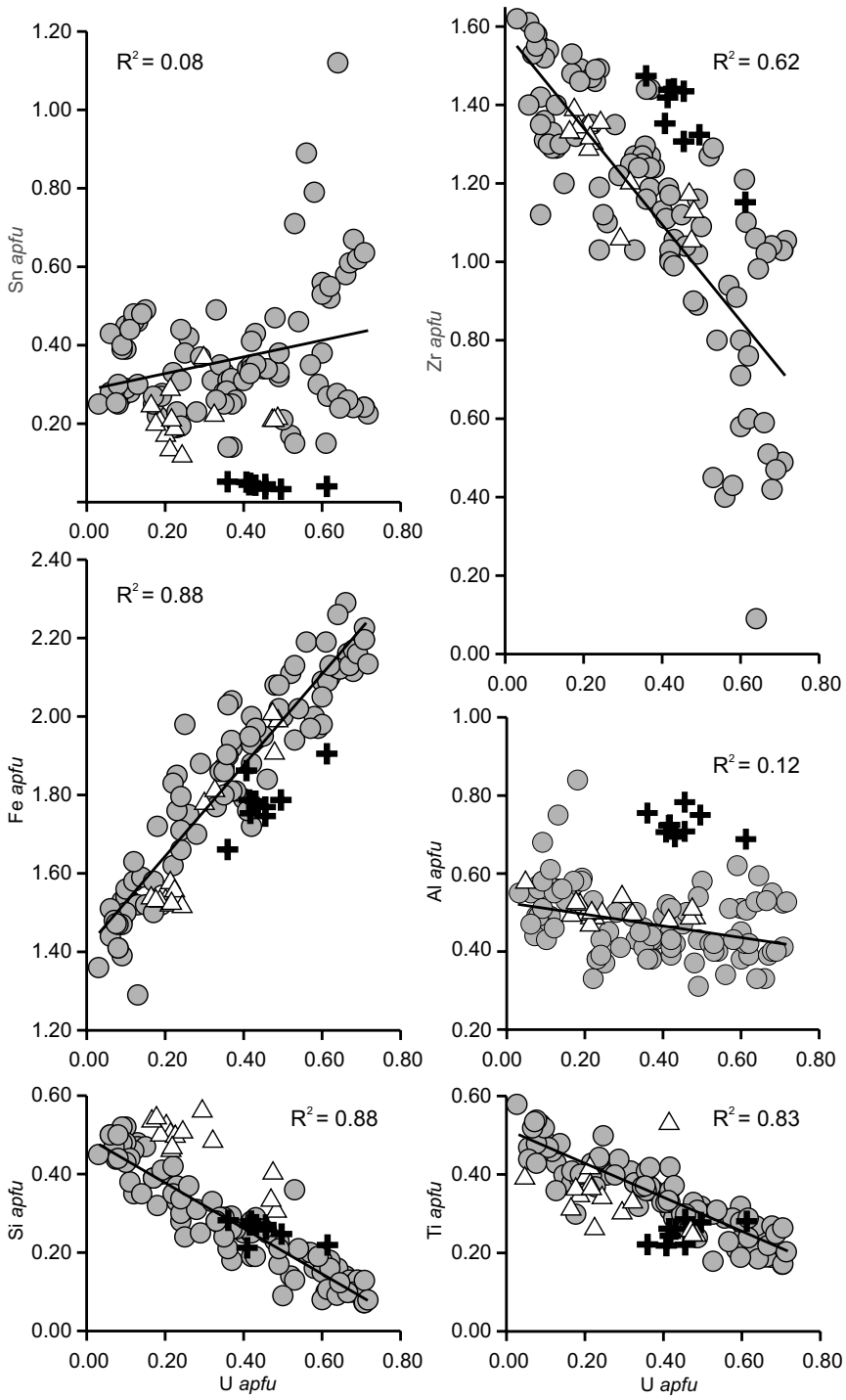

FIGURE 7. Correlation plots of U vs. Sn, Fe, Si, Zr, Al, Ti (apfu). R^2 is calculated for garnets of the xenolith 1 (100 analyses).

The refined structure of U-rich kimzeyite with ca. 10 wt% UO_3 (Table 2, analysis 15) must be interpreted in the context of the metamict character of the garnets. (1) The single-crystal diffraction pattern is considerably weaker and more diffuse than expected for a well-crystallized garnet of similar size and composition. (2) In spite of the strong difference in electrons (92 for U vs. 40 for Zr), population refinements for the octahedral Y site yielded site scattering of 40 electrons. The expected value based on electron microprobe analyses of the same crystal would be 45.23 electrons (reference: eight-coordinate site fully occupied by Ca). And (3) electron microprobe analyses suggest an average number of 21.55 scattering electrons on the tetrahedral Z site, whereas site occupation refinements converged to 20.1 electrons, modeled by Si (14 electrons) and Fe (26 electrons). The refined Z-O distance for the tetrahedron is 1.802(4) Å (Table 4[1]). A corresponding Z-O distance of 1.832 Å has been reported for a synthetic garnet of

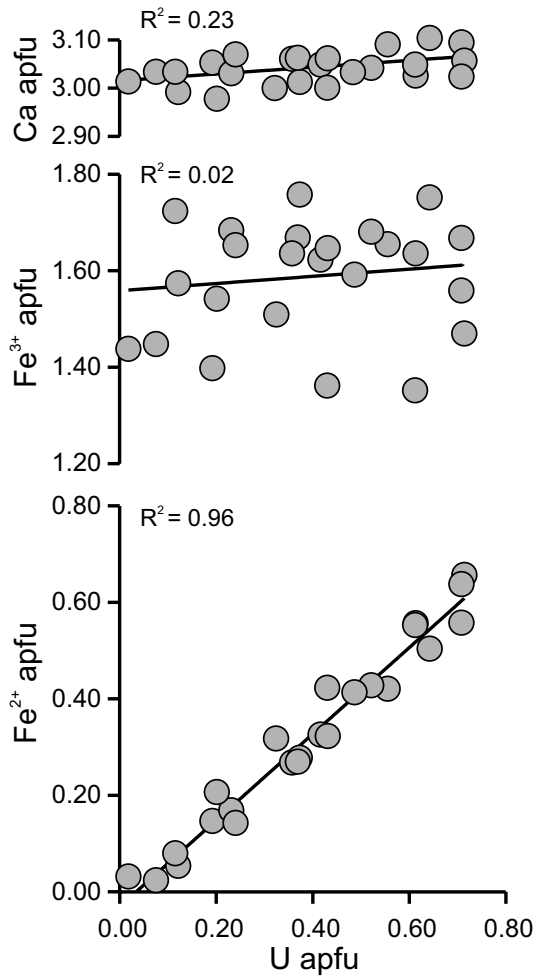

FIGURE 8. Correlation plots of U vs. Ca, Fe^{3+}, Fe^{2+} (apfu) (only analyses made on grains larger than 5 μm in size).

$Y_3(Fe^{3+}_{0.93}Al_{0.07})_2(Fe^{3+}_{0.72}Al_{0.28})_3O_{12}$ composition (Rodic et al. 2001). Variations in Z-O distances in these types of garnets are related mainly to variable Si, Al, Fe^{2+}, and Fe^{3+} content. Our single-crystal X-ray study on U-rich kimzeyite confirms that domains enriched in U are metamict and that they contribute only marginally to the diffraction pattern. This explains the poor agreement in scattering power for the octahedral site, while agreement for the tetrahedral site is good (Table 4[1]).

We suggest that primary non-metamict elbrusite-(Zr) has a composition very similar to the composition of the metamict phase analyzed in this paper with the electron microprobe (Table 2). Unambiguously, elbrusite-(Zr) is a member of the garnet group and shows a continuous solid solution with kimzeyite (Figs. 6 and 7). The small size of elbrusite-(Zr) crystals prohibits heating experiments to re-establish the original crystalline state. Furthermore, without knowledge of exact formation conditions (T, P, f_{O_2}), there is also a high probability that, under arbitrary heating conditions, the garnet transforms to unwanted decomposition products.

Elbrusite-(Zr) and other Sn-Zr-Sb-garnets formed as a result of high-temperature contact alteration of carbonate xenoliths during the explosive eruption of persilic 2.8 Ma ignimbrites at 800–1000 °C and low pressure, corresponding to the larnite facies of contact metamorphism (Gazeev et al. 2006; Galuskin et al. 2008, 2009). Accessory zircon from the ignimbrites of the Upper Chegem volcanic structure is the most likely U and Zr source for elbrusite-(Zr). The possibility that the zircon was a detrital component of the sedimentary protholith of the skarns cannot be ruled out. The unusually high temperature of skarn formation and the association of elbrusite-(Zr) with rock-forming minerals containing CO_3, Cl, and F suggest high U mobility during the metasomatic alteration of the primary xenoliths. Taking into account the toturite and bitikleite series data of Galuskina et al. (2010a, 2010b), the following sequence of high-temperature garnet crystallization in the spurrite zones of the skarned xenoliths is proposed: kimzeyite → elbrusite-(Zr) → "elbrusite-(Sn)" and, in the cuspidine (larnite) zone: kimzeyite → elbrusite-(Zr) → "elbrusite-(Sn)" → toturite → bitikleite-(ZrFe) and bitikleite-(SnAl).

Elbrusite-(Zr) with 20–27 wt% of UO_3 (Table 2) formed ca. 2.8 Ma years ago (Lipman et al. 1993; Gazis et al. 1995). Hence, this garnet is an ideal model substance to investigate problems concerning potential use of garnet matrices for immobilization of high-level radioactive waste. Up to now, absence of natural garnets with significant U and Th contents forced researchers to use synthetic materials to study the substitution capacity, as well as behavior and stability of garnet matrices as potential materials for immobilization of actinides (Burakov et al. 2000; Yudintsev et al. 2002, 2007; Yudintsev 2003; Livshits and Yudintsev 2008; Laverov et al. 2010). Utsunomiya with co-authors (Utsunomiya et al. 2002a, 2002b, 2005) investigated the radiation susceptibility of garnet matrices both natural silicate garnets and synthetic garnets of different composition irradiated with 1 MeV Kr^{2+} ions. Besides, garnets containing the short-living isotope ^{244}Cm were synthesized allowing estimation of the critical amorphization dose of a garnet matrix (Lukinykh et al. 2008). All known experiments give very close values of dpa 0.17–0.22 for both natural silicate garnets and synthetic ferrigarnets. Our preliminary data show, that uranian kimzeyite with 15.13 wt% UO_3 and calculated dpa 0.21 (Table 2) preserved the crystal structure as confirmed by the well-defined EBSD pattern (Fig. 3b). In contrast, elbrusite-(Zr) with calculated dpa 0.35 is nearly completely metamict (Fig. 3a), whereas U-bearing lakargiite (7.41 wt% UO_3) associated with elbrusite-(Zr) (Fig. 2b) and calculated dpa of 0.03, gives an EBSD pattern with distinct Kikuchi lines (Fig. 3c) indicating low degree of metamictization. The calculated cumulative dose for lakargiite is actually underestimated because the α-decay damage effect of adjacent elbrusite-(Zr) was not considered.

We plan to study the crystallinity of kimzeyite–elbrusite-(Zr) series garnet with different UO_3 concentrations to estimate the critical amorphization doses of Ca-Zr-ferrite type garnet matrices. μXRD powder diffraction data of lakargiite–U-bearing kimzeyite aggregates (Fig. 2; Table 2, analysis 13: 17.23 wt% UO_3, dpa 0.24) indicate partial preservation of the garnet and lakargiite structure (Fig. 4[1], supplementary material[1]). The critical amorphization dose dpa for elbrusite-(Zr) is about 0.25–0.30 and this range is higher than 0.17–0.22 dpa determined for synthetic garnet matrices (Utsunomiya et al. 2005) and for natural silicate garnets (Utsunomiya et al. 2002a). Synthetic ferrigarnet materials are considered as perspective matrices for the immobilization of high-level radioactive waste (Yudintsev 2003; Laverov et al. 2010). Our investigations on uranian elbrusite-(Zr) confirm the high radiation stability of the garnet structure.

ACKNOWLEDGMENTS

The authors thank to anonymous reviewers for their careful revision that improved the early version of the manuscript. The work was partly supported by the Russian Foundation of Basic Researches, Project 08-05-00181. I.G. and E.G. acknowledge support by the Ministry of Science and Higher Education of Poland, grants N N307 097038 and N N307 100238, respectively.

REFERENCES CITED

Allen, G.C. and Griffiths, A.J. (1979) Vibrational spectroscopy of alkaline-earth metal urinate compounds. Journal of the Chemistry Society, Dalton Transaction, 315–319.

Borsuk, A.M. (1968) Kainozoic magmatism. Geologia SSSR, T. IX. Northern Caucasus. Part I, 539–545.

Burakov, B.E., Anderson, E.B., Zamoryanskaya, M.V., and Petrova, M.A. (2000) Synthesis and study of ^{239}Pu-doped gadolinium-aluminium garnet. In B.E. Burakov and A.S. Aloy, Eds., Scientific Basis for Nuclear Waste Management XXXIII, 608, p. 419–422. Material Resources Society, Symposium Proceedings 1193, Warrendale, Pennsylvania.

Ewing, R.C., Meldrum, A., Wang, L., and Wang, S. (2000) Radiation-induces amorphisation. In S.A.T. Redfern and M.A. Carpenter, Eds., Transfromation Process in Minerals, 39, p. 319–361. Review in Mineralogy and Geochemistry, Mineralogical Society of America, Chantilly, Virginia.

Frost, R.L., Čejka, J., Weier, M.L., and Martens, W. (2006) A Raman and infrared spectroscopic study of the uranyl silicates—Weeksite, soddyite and haiweeite: Part 2. Spectrochimica Acta Part A, 63, 305–312.

Galuskin, E.V., Gazeev, V.M., Armbruster, T., Zadov, A.E., Galuskina, I.O., Pertsev, N.N., Dzierżanowski, P., Kadiyski, M., Gurbanov, A.G., Wrzalik, R., and Winiarski, A. (2008) Lakargiite $CaZrO_3$: a new mineral of the perovskite group from the North Caucasus, Kabardino-Balkaria, Russia. American Mineralogist, 93, 1903–1910.

Galuskin, E.V., Gazeev, V.M., Lazic, B., Armbruster, T., Galuskina, I.O., Zadov, A.E., Pertsev, N.N., Wrzalik, R., Dzierzanowski, P., Gurbanov, A.G., and Bzowska, G. (2009) Chegemite $Ca_7(SiO_4)_3(OH)_2$—a new humite-group calcium mineral from the Northern Caucasus, Kabardino-Balkaria, Russia. European Journal of Mineralogy, 21, 1045–1059.

Galuskina, I.O., Galuskin, E.V., Dzierżanowski, P., Armbruster, Th., and Kozanecki, M. (2005) A natural scandian garnet. American Mineralogist, 90, 1688–1692.

Galuskina, I.O., Galuskin, E.V., Dzierżanowski, P., Gazeev, V.M., Prusik, K., Pertsev, N.N., Winiarski, A., Zadov, A.E., and Wrzalik, R. (2010a) Toturite $Ca_3Sn_2Fe_2SiO_{12}$—A new mineral species of the garnet group. American Mineralogist, 95, 1305–1311.

Galuskina, I.O., Galuskin, E.V., Armbruster, T., Lazic, B., Dzierżanowski, P., Gazeev, V.M., Prusik, K., Pertsev, N.N., Winiarski, A., Zadov, A.E., Wrzalik, R., and Gurbanov, A.G. (2010b) Bitikleite-(SnAl) and bitikleite-(ZrFe)—new garnets from xenoliths of the Upper Chegem volcanic structure, Kabardino-Balkaria, Northern Caucasus, Russia. American Mineralogist, 95, 959–967.

Gaspar, M., Knaack, C., Meinert, L.D., and Moretti, R. (2008) REE in skarn systems: A LA-ICP-MS study of garnets from the Crown Jewel gold deposit. Geochimica et Cosmochimica Acta, 72, 185–205.

Gazeev, V.M., Zadov, A.E., Gurbanov, A.G., Pertsev, N.N., Mokhov, A.V., and Dokuchaev, A.Ya. (2006) Rare minerals of Verkhniy Chegem caldera (in skarned carbonate xenoliths in ignimbrites). Vestnik Vladikavkazskogo Nauchnogo Centra, 6, 18–27 (in Russian).

Gazis, C.A., Lanphere, M., and Taylor, H.P. (1995) $^{40}Ar/^{39}Ar$ and $^{18}O/^{16}O$ studies of the Chegem ash-flow caldera and the Eldjurta Granite: Cooling of two Pliocene igneous bodies in the Greater Caucasus Mountains, Russia. Earth and Planetary Science Letters, 134, 377–391.

Hatert, F. and Burke, E.A.J. (2008) The IMA–CNMNC dominant-constituent rule revisited and extended. Canadian Mineralogist, 46, 717–728.

Hoekstra, H.R. (1965) Infrared spectra of some alkali metal uranates. Journal of Inorgonic and Nuclear Chemistry, 27, 801–808.

Kolesov, B.A. and Geiger, C.A. (1998) Raman spectra of silicate garnets. Physics and Chemistry of Minerals, 25, 142–151.

Koopmans, H.J.A., van de Velde, G.M.H., and Gellings, P.J. (1983) Powder neutron diffraction study of the perovskites $CaTiO_3$ and $CaZrO_3$. Acta Crystallographica, C39, 1323–1325.

Laverov, N.P., Yudintsev, S.V., Livshits, T.S., Stefanovsky, S.V., Lukinykh, A.N., and Ewing, R.C. (2010) Synthetic minerals with the pyrochlore and garnet structures for immobilisation of actinide-containing waste. Geochemistry International, 48, 1–14.

Levinson, A.A. (1966) A system of nomenclature for rare earth minerals. American Mineralogist, 51, 152–158.

Liegeois-Duyckaerts, M. (1977) Infrared and Raman spectrum of $CaUO_4$: New data and interpretation. Spectrochimica Acta Part A, Molecular Spectroscopy, 6–7, 709–713.

Lipman, P.W., Bogatikov, O.A, Tsvetkov, A.A., Gazis, A.G., Gurbanov, A.G., Hon, K., Koronovsky, N.V., Kovalenko, V.I., and Marchev, P. (1993) 2.8 Ma ash-flow caldera at Chegem River in the northern Caucasus Moutains (Russia): contemporaneous granites, and associated ore deposits. Journal of Volcanology and Geothermal Research, 57, 85–124.

Livshits, T.S. and Yudintsev, S.V. (2008) Natural and synthetic minerals—matrices (forms) for actinide waste immobilization. In S. Krivovichev, Ed., Minerals as Advanced Materials, p. 193–207. Springer, Berlin.

Lukinykh, A.N., Tomilin, S.V., Lizin, A.A., and Livshits, T.S. (2008) Radiation and chemical resistance of synthetic ceramics based on ferritic garnet. Radiokhimiya, 50, 375–379.

Lupini, L., Williams, C.T., and Woolley, A.R. (1992) Zr-rich garnet and Zr- and Th-rich perovskite from the Polino carbonatite, Italy. Mineralogical Magazine, 56, 581–586.

Rodic, D., Mitric, M., Tellgren, R., and Rundlof, H. (2001) The cation distribution and magnetic structure of $Y_3Fe_{5-x}Al_xO_{12}$. Journal of Magnetism and Magnetic Materials, 232, 1–8.

Rusakov, V.S., Urusov, V.S., Kovalchuk, R.V., Kabalov, Y.K., and Yudincev, S.V. (2005) Mössbauer study of ferrite-garnets as matrixes for disposal of highly radioactive waste products. Hyperfine Interactions, 164, 99–104.

Shannon, R.D. (1976) Revised effective ionic radii and systematic studies of interatomic distances in halides and chalcogenides. Acta Crystallographica, A32, 751–767.

Schingaro, E., Scordari, F., Capitano, F., Parodi, G., Smith, D.S., and Mottana, A. (2001) Crystal chemistry of kimzeyite from Anguillara, Mts. Sabatini, Italy. European Journal of Mineralogy, 13, 749–759.

Smith, M.P., Henderson, P., Jeffries, T.E.R., Long, J., and Williams, C.T. (2004) The rare earth elements and uranium in garnets from the Beinn an Dubhaich Aureole, Skye, Scotland, U.K.: Constraints on Processes in a Dynamic Hydrothermal System. Journal of Petrology, 45, 457–484.

Strocka, B., Holst, P., and Tolksdorf, W. (1978) An empirical formula for the calculation of lattice constants of oxides garnets based on substituted yttrium- and gadolinium-iron garnets. Philips Journal of Research, 33, 186–202.

Utsunomiya, S., Wang, L.M., and Ewing, R.C. (2002a) Ion irradiation effects in natural garnets: comparison with zircon. Nuclear Instruments and Methods in Physics Research, B191, 600–605.

Utsunomiya, S., Wang, L.M., Yudintsev, S., and Ewing, R.C. (2002b) Ion irradiation-induced amorphization and nano-crystal formation in garnets. Journal of Nuclear Materials, 303, 177–187.

Utsunomiya, S., Yudintsev, S., and Ewing R.C. (2005) Radiation effects in ferrate garnet. Journal of Nuclear Materials, 336, 251–260.

Wülser, P.-A., Meisser, N., Brugger, J., Schenk, K., Ansermet, S., Bonin, M., and Bussy, F. (2005) Cleusonite, $(Pb,Sr)(U^{4+},U^{6+})(Fe^{2+},Zn)_2(Ti,Fe^{2+},Fe^{3+})_{18}(O,OH)_{38}$, a new mineral species of the crichtonite group from western Swiss Alps. European Journal of Mineralogy, 17, 933–942.

Yudintsev, S.V. (2003) Structure-chemical approaches to selection of crystal matrix for immobilization of actinoids. Geology of Ore Deposits, 45, 172–187.

Yudintsev, S.V., Lapina, M.I., Ptashkin, A.G., Ioudintseva, T.S., Utsunomiya, S., Wang, L.M., and Ewing, R.C. (2002) Accommodation of uranium into the garnet structure. Material Research Society Symposium Proceedings, 713, 477–480.

Yudintsev, S.V., Stefanovsky, S.V., and Ewing, R.C. (2007) Actinide host phases as radioactive waste forms. In S.V. Krivovichev, P.C. Burns, and I.G. Tananaev, Eds., Structural Chemistry of Inorganic Actinide Compounds, p. 453–490. Elsevier, Amsterdam.

MANUSCRIPT RECEIVED JANUARY 20, 2010
MANUSCRIPT ACCEPTED APRIL 1, 2010
MANUSCRIPT HANDLED BY DANIEL HARLOV